Few-Body Systems 36, 5–12 (2005)
DOI 10.1007/s00601-004-0074-y

Few-Body Systems
Printed in Austria

Progress on Calorons and Their Constituents*

F. Bruckmann, D. Nógrádi, and P. van Baal

Instituut-Lorentz for Theoretical Physics, University of Leiden,
P.O. Box 9506, NL-2300 RA Leiden, The Netherlands

Received October 1, 2004; accepted November 11, 2004
Published online April 4, 2005;

Abstract. We review the recent progress made in understanding instantons at finite temperature (calorons) with non-trivial holonomy, and their monopole constituents as relevant degrees of freedom for the confined phase.

1 Introduction

There has been a revived interest in studying instantons at finite temperature T, so-called calorons [1, 2]. The main reason is that new explicit solutions could be obtained in the case where the Polyakov loop at spatial infinity (the so-called holonomy) is non-trivial, necessary to reveal more clearly the monopole constituent nature of these calorons [3, 4]. Trivial holonomy, i.e., with values in the centre of the gauge group, is typical for the deconfined phase. Non-trivial holonomy is therefore expected to play a role in the confined phase (i.e., for $T < T_c$) where the trace of the Polyakov loop fluctuates around small values. The properties of instantons are therefore directly coupled to the order parameter for the deconfining phase transition.

At finite temperature A_0 plays in some sense the role of a Higgs field in the adjoint representation, which explains why magnetic monopoles occur as constituents of calorons. Since A_0 is not necessarily static it is better to consider the Polyakov loop as the analog of the Higgs field,

$$P(t,\boldsymbol{x}) = \mathrm{Pexp}\left[\int_0^\beta A_0(t+s,\boldsymbol{x})\,ds\right], \tag{1}$$

which, like an adjoint Higgs field, transforms under a periodic gauge transformation $g(x)$ to $g(x)P(x)g^{-1}(x)$. Here $\beta = 1/kT$ is the period in the imaginary time direction, under which the gauge field is assumed to be periodic. Finite action

* Presented by the last author at Light-Cone 2004, Amsterdam, The Netherlands, August 16–20, 2004

requires the Polyakov loop at spatial infinity to be constant. For $SU(n)$ gauge theory this gives

$$\mathcal{P}_\infty = \lim_{|\boldsymbol{x}|\to\infty} P(0,\boldsymbol{x}) = g^\dagger \exp[2\pi i\,\mathrm{diag}(\mu_1,\mu_2,\ldots,\mu_n)]\,g, \tag{2}$$

where g is chosen to bring $\mathcal{P}_\infty$ to its diagonal form, with the n eigenvalues being ordered according to

$$\sum_{i=1}^{n}\mu_i = 0, \qquad \mu_1 \le \mu_2 \le \cdots \le \mu_n \le \mu_{n+1} \equiv 1+\mu_1. \tag{3}$$

In the algebraic gauge (used in constructing solutions), where $A_0(x)$ is transformed to zero at spatial infinity, the gauge fields satisfy the boundary condition

$$A_\mu(t+\beta,\boldsymbol{x}) = \mathcal{P}_\infty A_\mu(t,\boldsymbol{x})\mathcal{P}_\infty^{-1}. \tag{4}$$

Caloron solutions are such that the total magnetic charge vanishes. A single caloron with topological charge one contains $n-1$ monopoles with a unit magnetic charge in the i-th $U(1)$ subgroup, which are compensated by the n-th monopole of so-called type $(1,1,\ldots,1)$, having a magnetic charge in each of these subgroups [5]. At topological charge k there are kn constituents, k monopoles of each of the n types. The monopole of type j has a mass $8\pi^2\nu_j/\beta$, with $\nu_j \equiv \mu_{j+1}-\mu_j$. The sum rule $\sum_{j=1}^{n}\nu_j = 1$ guarantees the correct action, $8\pi^2 k$, for calorons with topological charge k.

Prior to their explicit construction, calorons with non-trivial holonomy were considered irrelevant [2], because the one-loop correction gives rise to an infinite action barrier. However, the infinity simply arises due to the integration over the finite energy density induced by the perturbative fluctuations in the background of a non-trivial Polyakov loop [6]. Recently the calculation of the non-perturbative contribution was performed [7]. When added to this perturbative contribution, with minima at centre elements, these minima turn unstable for decreasing temperature right around the expected value of T_c. This lends some support to monopole constituents being the relevant degrees of freedom which drive the transition from a phase in which the centre symmetry is broken at high temperatures to one in which the centre symmetry is restored at low temperatures. Lattice studies, both using cooling [8] and chiral fermion zero-modes [9] as filters, have also conclusively confirmed that monopole constituents do dynamically occur in the confined phase.

2 Properties of Caloron Solutions

Well-separated constituents can be shown to act as point sources for the so-called far field, that is far removed from any of the cores, where the gauge field is Abelian [10]. When constituents of opposite charge (n constituents of different type) come together, the action density no longer deviates significantly from that of a standard instanton. Its scale parameter ρ is related to the constituent separation d through $\pi\rho^2/\beta = d$. A typical example for a charge-1 $SU(2)$ caloron with far and nearby constituents is shown in Fig. 1 (left). When $\rho \ll \beta$ no difference would be seen with the Harrington-Shepard solution [1], the gauge field is nevertheless vastly

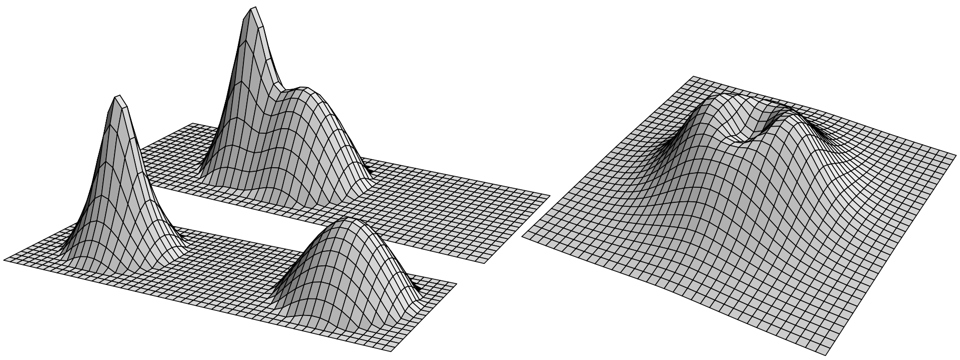

Fig. 1. On the left are shown two charge-1 $SU(2)$ caloron profiles at $t=0$ with $\beta=1$ and $\mu_2=-\mu_1=0.125$, for $\rho=1.6$ (bottom) and 0.8 (top) on equal logarithmic scales, cut off below an action density of $1/(2e^2)$. On the right we show the action density (on a linear scale) of a typical $SU(2)$ caloron with topological charge 2 and $\mu_2=-\mu_1=0.25$ for which two constituents of equal magnetic charge are closer than their individual sizes (but not exactly on top). When the other two constituents are far away, as for the case shown here, this becomes a charge-2 monopole solution

different, as follows from the fact that within the confines of the peak there are n locations where two of the eigenvalues of the Polyakov loop coincide [11]. When, on the other hand, constituents of equal charge come together (which requires $k>1$), an extended core structure appears [10]. For two coinciding constituents this gives rise to the typical doughnut structure also observed for monopoles [12], see Fig. 1 (right).

2.1 Fermion Zero-Modes

An essential property of calorons is that the chiral fermion zero-modes are localized to constituents of a certain charge only. The latter depends on the choice of a boundary condition for the fermions in the imaginary time direction (allowing for an arbitrary $U(1)$ phase $\exp[2\pi iz]$) [13]. This provides an important signature for the dynamical lattice studies, using chiral fermion zero-modes as a filter [9]. To be precise, the zero-modes are localized to the monopoles of type m provided $\mu_m<z<\mu_{m+1}$ (most of the time we use the classical scale invariance to set $\beta=1$). Denoting the zero-modes by $\hat{\Psi}_z^a(x)$, where $a=1,\ldots,k$ for a caloron of topological charge k, we can write

$$\hat{\Psi}_z^a(x)^\dagger\hat{\Psi}_z^b(x)=-(2\pi)^{-2}\partial_\mu^2\hat{f}_x^{ab}(z,z), \tag{5}$$

where $\hat{f}^{ab}(z,z')$ is a Green's function that appears in the construction to be discussed below. The trace, i.e., the sum over the zero-mode densities, has a remarkably simple form in the far field limit (denoted by ff and defined by neglecting terms that decay exponentially with the distance to any of the constituent cores)

$$\mathrm{Tr}\hat{f}_x^{\mathrm{ff}}(z,z)=4\pi^2\mathcal{V}_m(\boldsymbol{x}), \qquad \text{for} \quad \mu_m<z<\mu_{m+1}. \tag{6}$$

As is implicit in the notation, $\mathcal{V}_m$ is static and independent of z within its interval of definition. In addition $\mathcal{V}_m$ has to be harmonic (up to singularities), because the zero-modes decay exponentially as long as $z \neq \mu_j$ (for any j), and therefore do not survive in the far field limit. For $k = 1$ and $\boldsymbol{y}_m$ the constituent location one simply has $\mathcal{V}_m(\boldsymbol{x}) = 1/(4\pi|\boldsymbol{x} - \boldsymbol{y}_m|)$, whereas for $k = 2$ we found [10]

$$\mathcal{V}_m(\boldsymbol{x}) = \frac{1}{2\pi|\boldsymbol{x}|} + \frac{\mathcal{D}}{4\pi^2}\int_{r<\mathcal{D}} dr\, d\varphi \frac{\partial_r|\boldsymbol{x} - r\boldsymbol{y}(\varphi)|^{-1}}{\sqrt{\mathcal{D}^2 - r^2}}, \tag{7}$$

where $\boldsymbol{y}(\varphi) = (\sqrt{1-\mathbf{k}^2}\cos\varphi, 0, \sin\varphi)$, up to an arbitrary coordinate shift and rotation. Here $\mathcal{D}$ is a scale and $\mathbf{k}$ a shape parameter to characterize *arbitrary* $SU(2)$ charge-2 solutions. In this representation it is clear that $\mathcal{V}_m(\boldsymbol{x})$ is harmonic everywhere except on a disk bounded by an ellipse with minor axes $2\mathcal{D}\sqrt{1-\mathbf{k}^2}$ and major axes $2\mathcal{D}$. Although not directly obvious, when $\mathbf{k} \to 1$ the support of the singularity structure is on two points only, separated by a distance $2\mathcal{D}$. Taking an arbitrary test function $f(\boldsymbol{x})$ one can prove that [10]

$$-\lim_{\mathbf{k}\to 1}\int f(\boldsymbol{x})\partial_i^2\mathcal{V}_m(\boldsymbol{x})\, d^3x = f(0,0,\mathcal{D}) + f(0,0,-\mathcal{D}). \tag{8}$$

Monopoles of different charges have to adjust to each other to form an exact caloron solution, such that $\mathbf{k}$ and $\mathcal{D}$ are in general not independent. So far we constructed two classes of solutions illustrated in Fig. 2 for both of which a large value of $\mathcal{D}$ implies that $\mathbf{k}$ approaches 1 exponentially. Hence we find point-like constituents, a necessary requirement to describe the field configurations at larger distances in terms of these objects. When all constituents of other types are sent to infinity, we recover the exact multi-monopole solutions of a given type of magnetic charge, and our results therefore also provide explicit solutions for the monopole zero-modes, which were not known before for the multi-monopole configurations.

Surprisingly, the charge distribution that gives rise to the Abelian field far from any of the constituent cores (even when extended due to overlap) can be calculated

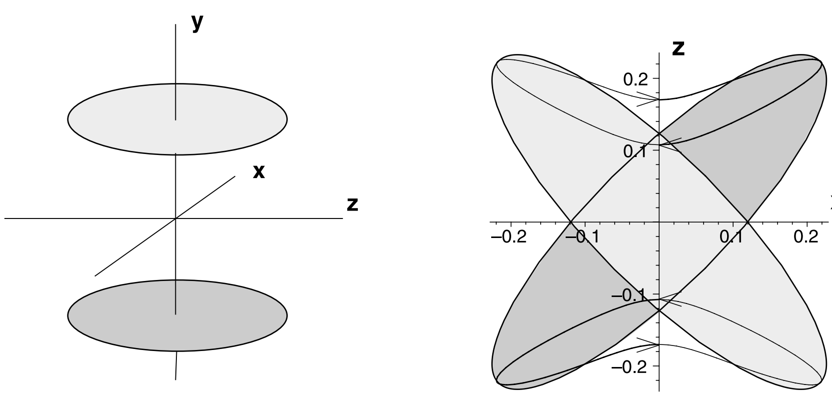

Fig. 2. Illustration of the location of the disk singularities (light and dark shaded according to magnetic charge) for a so-called "rectangular" (left) and "crossed" (right) configuration, as used for the $k = 2$ solutions shown in Fig. 1 and Fig. 3, respectively. The curves for the "crossed" case represent a one-parameter family of solutions interpolating between two axially symmetric solutions for which $\mathbf{k} = 1$ independent of $\mathcal{D}$, giving point-like constituents without the need to take $\mathcal{D}$ large. See ref. [10] for more details

exactly from $\mathcal{V}_m(\boldsymbol{x})$. We consider here $SU(2)$, for which we can parametrize the holonomy by $\mathcal{P}_\infty = \exp[2\pi i\boldsymbol{\omega}\cdot\boldsymbol{\tau}]$ ($\mu_2 = -\mu_1 = |\boldsymbol{\omega}|$), where τ_a are the usual Pauli matrices. The field asymptotically becomes Abelian, and is necessarily proportional to $\hat{\omega}\cdot\boldsymbol{\tau}$. Hence $A_0^{\rm ff}(\boldsymbol{x}) = 2\pi i\boldsymbol{\omega}\cdot\boldsymbol{\tau} - \frac{1}{2}i\hat{\omega}\cdot\boldsymbol{\tau}\Phi(\boldsymbol{x})$, where the constant term (absent in the algebraic gauge) shows again how A_0 plays the role of a Higgs field. We found for $k=1$ and 2 that $\Phi(\boldsymbol{x}) = 2\pi(\mathcal{V}_1(\boldsymbol{x}) - \mathcal{V}_2(\boldsymbol{x}))$. Therefore, the singularity structure in the zero-mode density agrees *exactly* with the Abelian charge distribution, as given by $\partial_i^2\Phi(\boldsymbol{x})$. Since the electric field is given in terms of the gradient of A_0, which due to the self-duality is equal to the magnetic field, a particularly simple formula results for the action density $\mathcal{S}$. Using in addition that outside the cores there is no source for the Abelian field, implying A_0 to be harmonic in the far field (as is also clear from the relation to $\mathcal{V}_m$), we find

$$\mathcal{S}^{\rm ff}(\boldsymbol{x}) = -2\,{\rm tr}(\partial_i A_0(\boldsymbol{x}))^2 = 2\partial_i^2\,{\rm tr}\,A_0^2(\boldsymbol{x}) = -\partial_i^2\Phi^2(\boldsymbol{x}). \tag{9}$$

The algebraic tail of the action density is thus known to all orders in $1/|\boldsymbol{x}|$, which is of course equivalent to the fact that the charge distribution, $\partial_i^2\Phi(\boldsymbol{x})$, giving rise to this asymptotic field is also exactly known, even though the formula for the action density can of course only be used outside any of the constituent cores.

3 The Construction – in Brief

Our construction of caloron solutions in its practical implementation relies heavily on the Atiyah-Drinfeld-Hitchin-Manin construction [14] of multi-instantons and on the closely related Nahm transformation [15]. For the $k=1$ Harrington-Shepard solution [1] one simply takes a periodic array of $\mathbb{R}^4$ instanton solutions, which can be easily constructed through the 't Hooft ansatz, provided the relative color orientation between subsequent periods is trivial. This necessarily gives trivial holonomy. Here the algebraic gauge discussed earlier is useful, as it shows that with non-trivial holonomy, shifting over each period the gauge field rotates in color space by an amount exactly given by the holonomy. It necessitates the use of the full ADHM formalism. The crucial observation has been that the "twisted" shift symmetry lends itself very well to Fourier transformation and makes contact with the Nahm transformation for calorons [15]. The variable z we introduced in formulating the generalized boundary conditions for the chiral fermions is precisely the dual of t under this transformation.

To construct a charge k caloron with non-trivial holonomy we place k instantons in the time interval $[0,\beta[$, performing a color rotation with $\mathcal{P}_\infty$ for each shift of t over β (compare Eq. (4)). The Fourier transformation introduces singularities at $z=\mu_m$ through the powers of $\mathcal{P}_\infty$, as is seen from writing $\mathcal{P}_\infty = \sum_m e^{2\pi i\mu_m}P_m$ in terms of the n projectors P_m. The Fourier transformation also introduces $\hat{A}(z)$ as a $U(k)$ gauge field on a circle, which satisfies the Nahm equation

$$\frac{d}{dz}\hat{A}_j(z) + [\hat{A}_0(z),\hat{A}_j(z)] + \tfrac{1}{2}\varepsilon_{jkl}[\hat{A}_k(z),\hat{A}_l(z)] = 2\pi i\sum_m \delta(z-\mu_m)\rho_m^j, \tag{10}$$

where one has $2\pi\zeta_a^\dagger P_m\zeta_b \equiv \mathbb{1}_2\,\hat{S}_m^{ab} - \boldsymbol{\tau}\cdot\boldsymbol{\rho}_m^{ab}$, in terms of a two-component spinor ζ_b in the $\bar{n}$ representation of $SU(n)$.

A Green's function $\hat{f}_x(z,z') \equiv \hat{g}^\dagger(z) f_x(z,z')\hat{g}(z')$ is introduced, where $f_x(z,z')$ is defined through

$$\left\{-\frac{d^2}{dz^2} + V(z;\boldsymbol{x})\right\} f_x(z,z') = 4\pi^2 \mathbb{1}_k \delta(z-z'), \tag{11}$$

with

$$V(z;\boldsymbol{x}) \equiv 4\pi^2 \boldsymbol{R}^2(z;\boldsymbol{x}) + 2\pi \sum_m \delta(z-\mu_m) S_m, \qquad S_m \equiv \hat{g}(\mu_m)\hat{S}_m \hat{g}^\dagger(\mu_m),$$
$$R_j(z;\boldsymbol{x}) \equiv x_j - (2\pi i)^{-1} \hat{g}(z)\hat{A}_j(z)\hat{g}^\dagger(z). \tag{12}$$

Note that the S_m play the role of "impurities" and that

$$\hat{g}(z) \equiv \exp[2\pi i(\xi_0 - x_0 \mathbb{1}_k)z], \tag{13}$$

defined in terms of the dual holonomy $\exp[2\pi i \xi_0] \equiv \mathrm{Pexp}(\int_0^1 \hat{A}_0(z)\,dz)$, can be used to transform $\hat{A}_0 - 2\pi i x_0 \mathbb{1}_k$ to zero, in order to simplify as much as possible the Green's function equation. This is at the expense of introducing periodicity up to a gauge transformation. Although $\hat{f}_x(z,z')$ is periodic in z and z' with period 1 (for $\beta = 1$), $f_x(z,z')$ no longer is.

Given a solution for the Green's function, there are straightforward expressions for the gauge field [16] only involving the Green's function evaluated at the "impurity" locations and for the fermion zero-modes [10]. For the zero-mode density see Eq. (5). As an example we give the Green's function at $z' = z$, which formally can be expressed as (the x dependence of $\mathcal{F}_z$ is implicit)

$$f_x(z,z) = -4\pi^2((\mathbb{1}_{2k} - \mathcal{F}_z)^{-1})_{12},$$
$$\mathcal{F}_z \equiv \hat{g}^\dagger(1)\,\mathrm{Pexp}\int_z^{z+1} dw \begin{pmatrix} 0 & \mathbb{1}_k \\ V(w;\boldsymbol{x}) & 0 \end{pmatrix}, \tag{14}$$

where the $(1,2)$ component on the right-hand side of the first identity is with respect to the 2×2 block matrix structure. This has allowed us to find a particularly compact expression for the action density [16],

$$\mathcal{S}(x) \equiv -\tfrac{1}{2}\,\mathrm{tr}\,F^2_{\mu\nu}(x) = -\tfrac{1}{2}\partial^2_\mu \partial^2_\nu \log\det(ie^{-\pi i x_0}(\mathbb{1}_{2k} - \mathcal{F}_z)), \tag{15}$$

which can be shown to be independent of z.

The formal expression for $\mathcal{F}_z$ can be made more explicit by a decomposition into the "impurity" contributions T_m at $z = \mu_m$ and the "propagation" $H_m \equiv W_m(\mu_{m+1}, \mu_m)$ between μ_m and μ_{m+1}, with for $z, z' \in (\mu_m, \mu_{m+1})$

$$T_m \equiv \begin{pmatrix} \mathbb{1}_k & 0 \\ 2\pi S_m & \mathbb{1}_k \end{pmatrix}, \quad W_m(z,z') \equiv \begin{pmatrix} f_m^+(z) & f_m^-(z) \\ \frac{d}{dz} f_m^+(z) & \frac{d}{dz} f_m^-(z) \end{pmatrix} \begin{pmatrix} f_m^+(z') & f_m^-(z') \\ \frac{d}{dz} f_m^+(z') & \frac{d}{dz} f_m^-(z') \end{pmatrix}^{-1}, \tag{16}$$

$$\mathcal{F}_z = W_m(z,\mu_m) T_m H_{m-1} \cdots H_1 T_1 \hat{g}^\dagger(1) H_n T_n \cdots T_{m+1} H_m W_m(\mu_m, z). \tag{17}$$

The $k \times k$ matrices $f_m^\pm(z)$ are defined for $z \in (\mu_m, \mu_{m+1})$ and behave as $f_m^\pm(z) \to \exp[\pm 2\pi |\boldsymbol{x}|(z-\mu_m)\mathbb{1}_k] f_m^\pm(\mu_m)$ for $|\boldsymbol{x}| \to \infty$, where $f_m^\pm(\mu_m)$ can be arbitrary

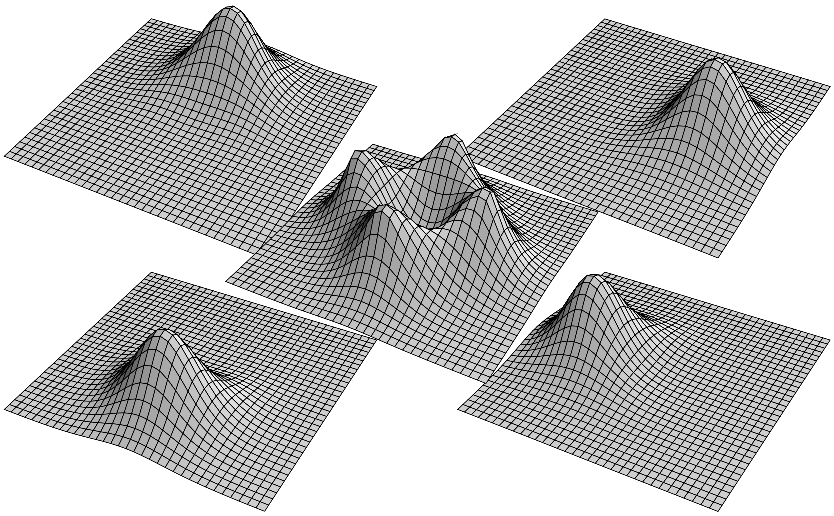

Fig. 3. In the middle is shown the action density in the plane of the constituents at $t = 0$ for an $SU(2)$ charge-2 caloron with $\mathrm{tr}\,\mathcal{P}_\infty = 0$ in the "crossed" configuration of Fig. 2, where all constituents strongly overlap. On a scale enhanced by a factor $10\pi^2$ are shown the densities for the two zero-modes, using either periodic (left) or anti-periodic (right) boundary conditions in the time direction. Note that these still are able to identify four individual constituents

non-singular matrices. Together these form the $2k$ solutions of the homogeneous Green's function equation,

$$\left(\frac{d^2}{dz^2} - 4\pi^2 \boldsymbol{R}^2(z;\boldsymbol{x})\right)\hat{v}(z;\boldsymbol{x}) = 0. \tag{18}$$

We have been able to use this "mix" of the ADHM and Nahm formalism both in making powerful approximations, like in the far field limit (based on our ability to identify the exponentially rising and falling terms), and for finding exact solutions through solving the homogeneous Green's function equation for $k = 2$.

What makes this case tractable is the fact that the Nahm equations on each interval can be solved in terms of elliptic functions [17]. For the caloron, apart from the axially symmetric solutions constructed in ref. [16], we found two sets of non-trivial solutions for the matching conditions that interpolate between overlapping and well-separated constituents, see Fig. 2. To resolve the full structure of the cores we had to find the exact solutions to Eq. (18). For this task we could make convenient use of an existing analytic result for charge-2 monopoles [18], adapting it to the case of calorons. Essential is that once the solutions $f_m^\pm(z)$ are known, everything else can be easily determined in terms of these (compare Eq. (17)). We conveniently expressed the explicit solutions for Eq. (18) in terms of the elliptic integral of the third kind, but refer to ref. [10] for further details. A sample of the results can be found in Fig. 1 (right) and Fig. 3.

4 Conclusions

We have seen that instantons at finite temperature are composed of constituent monopoles. Of course, the hope is to develop a calculational scheme to address questions like monopole condensation in the popular scenario of the dual superconductor [19]. However, this is very much complicated by the fact that at low temperature the coupling constant is large, and instantons form a dense ensemble. This does imply that the monopoles form a dense ensemble as well. One may then hope that the confining electric phase could be characterized by a dual deconfining magnetic phase, where the dual deconfinement is due to the large monopole density, similar in spirit to high density induced quark deconfinement.

References

1. Harrington, B. J., Shepard, H. K.: Phys. Rev. **D17**, 2122 (1978); Phys. Rev. **D18**, 2990 (1978)
2. Gross, D. J., Pisarski, R. D., Yaffe, L. G.: Rev. Mod. Phys. **53**, 43 (1981)
3. Kraan, T. C., van Baal, P.: Phys. Lett. **B428**, 268 (1998) [hep-th/9802049]; Nucl. Phys. **B533**, 627 (1998) [hep-th/9805168]
4. Lee, K.: Phys. Lett. **B426**, 323 (1998) [hep-th/9802012]; Lee, K., Lu, C.: Phys. Rev. **D58**, 025011 (1998) [hep-th/9802108]
5. Kraan, T. C., van Baal, P.: Phys. Lett. **B435**, 389 (1998) [hep-th/9806034]
6. Weiss, N.: Phys. Rev. **D24**, 475 (1981)
7. Diakonov, D., Gromov, N., Petrov, V., Slizovskiy, S.: Phys. Rev. **D70**, 036003 (2004) [hep-th/0404042]
8. Ilgenfritz, E.-M., Martemyanov, B. V., Müller-Preussker, M., Shcheredin, S., Veselov, A. I.: Phys. Rev. **D66**, 074503 (2002) [hep-lat/0206004]
9. Gattringer, C., Schaefer, S.: Nucl. Phys. **B654**, 30 (2003) [hep-lat/0212029]; Gattringer, C., Pullirsch, R.: Phys. Rev. **D69**, 094510 (2004) [hep-lat/0402008]
10. Bruckmann, F., Nógrádi, D., van Baal, P.: Nucl. Phys. **B666**, 197 (2003) [hep-th/0305063]; Nucl. Phys. **B698**, 233 (2004) [hep-th/0404210]
11. García Pérez, M., González-Arroyo, A., Montero, A., van Baal, P.: JHEP **06**, 001 (1999) [hep-lat/9903022]
12. Forgács, P., Horváth, Z., Palla, L.: Nucl. Phys. **B192**, 141 (1981)
13. García Pérez, M., González-Arroyo, A., Pena, C., van Baal, P.: Phys. Rev. **D60**, 031901 (1999) [hep-th/9905016]; Chernodub, M. N., Kraan, T. C., van Baal, P.: Nucl. Phys. Suppl. **B83–B84**, 556 (2000) [hep-lat/9907001]
14. Atiyah, M. F., Hitchin, N. J., Drinfeld, V., Manin, Yu. I.: Phys. Lett. **65A**, 185 (1978)
15. Nahm, W.: Self-Dual Monopoles and Calorons. In: Lecture Notes in Physics **201**, 189 (1984)
16. Bruckmann, F., van Baal, P.: Nucl. Phys. **B645**, 105 (2002) [hep-th/0209010]
17. Nahm, W.: Multi-Monopoles in the ADHM Construction. In: Gauge Theories and Lepton Hadron Interactions (Horváth, Z., et al., eds.). Budapest 1982; Brown, S. A., Panagopoulos, H., Prasad, M. K.: Phys. Rev. **D26**, 854 (1982)
18. Panagopoulos, H.: Phys. Rev. **D28**, 380 (1983)
19. Mandelstam, S.: Phys. Rept. **23**, 245 (1976); 't Hooft, G.: In: High-Energy Physics (Zichichi, A., ed.). Bologna 1976; Nucl. Phys. **B138**, 1 (1978)